Current Opinion in Solid State & Materials Science 23 (2019) 129–141

Contents lists available at ScienceDirect

Current Opinion in Solid State & Materials Science

journal homepage: www.elsevier.com/locate/cossms

Revisiting the effects of molybdenum and tungsten alloying on corrosion behavior of nickel-chromium alloys in aqueous corrosion

K. Lutton Cwalina, C.R. Demarest, A.Y. Gerard, J.R. Scully*

Center for Electrochemical Science and Engineering, Department of Materials Science and Engineering, University of Virginia, USA

ARTICLE INFO

Keywords:
Passivation
Corrosion
Molybdenum
Tungsten

ABSTRACT

Minor alloying additions such as molybdenum (Mo) have major effects on the localized corrosion resistance of corrosion resistant alloys containing chromium. However, progress in alloy development is mostly based upon empirical observations, where any mechanistic insights are largely relegated to the latter stages of localized corrosion (i.e., stabilization and propagation) that are more readily accessible experimentally. For instance, it is well understood that Mo and tungsten (W) affect repassivation of local active, as well as widespread transpassive, corrosion sites and Mo surface enrichment during corrosion is well-documented. In this paper, a comprehensive examination of the functions and mechanism by which selected Mo and W operate to improve the passivity and resistance to breakdown during the initial stages of localized corrosion of the most common Ni-based solid solution alloys is presented. It is shown that Mo and W exert considerable influence on many stages of corrosion, including both passivation and film breakdown, re-enforcing old and introducing more recent ideas in this comprehensive review of the current state of corrosion research on Ni-Cr-(Mo + W) alloys.

1. Introduction

Nickel and nickel-based alloys are structural materials of choice in a variety of aggressive corrosive and high temperature environments. They are superior to stainless steels in terms of corrosion resistance and high temperature stability in environments which historically create vulnerabilities for steels. These include strong, concentrated reducing acids, chloride-containing environments, certain molten salts, and hydrofluoric acids [1]. There are various classes of nickel alloys, including many single phase, solid solution materials such as Ni-Cu, Ni-Mo, Ni-Cr, Ni-Cr-Mo, Ni-Cr-Fe, and Ni-Cr alloys produced in many product forms [1]. These alloys are typically rich in Ni and contain one or more major solute alloying elements and sometimes minor alloying additions as well. This review paper focuses on single phase, solid solution nickel-base alloys that are highly resistant to localized corrosion in high temperature chemical process environments and when exposed to near room temperature aqueous, chloride-containing solutions. This stability is mainly attributed to a profound benefit of alloying with low concentrations of Mo and W in combination with Cr [2–6]. The exact mechanisms of this benefit are controversial and not completely understood.

Ni-Cr, Ni-Cr-Mo, and Ni-Cr-Mo-W solid solution alloys are highly corrosion resistant in a number of natural and industrial environments [7]. Ni-Cr alloys alloyed with increasing concentrations of Cr produce stable passive films that persist in harsh aqueous environments [8]. A significant amount of literature has been developed for various applications, e.g. marine [9], nuclear waste repositories [10], and in numerous environments of importance to the chemical process industry, such as concentrated HCl containing Fe^{3+} impurities [11]. These studies largely focus on corrosion rate dependencies associated with effects of alloying and structure in these select applications and environments. Prior understandings of the mechanisms generally fall into two broad camps or categories: passivity improved by a critical concentration of Cr plus minor amounts of Mo and/or W or repassivation at active localized corrosion sites [12–14]. Most studies within the former category focus on compositional, electronic, and physical attributes of the oxide such as the passive film thickness, structure, and descriptions of passivating layers. For instance, Mo is thought to exist as Mo(IV) in inner layers while Mo(VI) is present in an outer, cation-selective layer on Fe-Cr-Mo alloys [15,16]. Similar layering has been proposed for Ni-Cr-Mo alloys [12,17]. In contrast, most studies concerning the latter stage of corrosion focus on critical temperature, critical potentials, and crevice geometry–dissolution rate parameters which indicate thresholds for crevice attack versus repassivation [18–20]. These phenomena are associated with crevice sites and geometric crevice formers at the micrometer scale [21] and often consider how Mo and W surface

* Corresponding author.
E-mail address: jrs8d@virginia.edu (J.R. Scully).

https://doi.org/10.1016/j.cossms.2019.03.002
Received 7 August 2018; Received in revised form 4 March 2019; Accepted 18 March 2019
Available online 26 March 2019
1359-0286/

enrichments affect these processes. This distinction is important because the former focuses on benefits conferred within a nm thick oxide film while the later focuses on phenomena at active corrosion sites. A gap in understanding exists because descriptions of oxide characteristics fall short of directly linking atomic scale details of how alloying elements such as Mo and W effect passivity and suppress trigger events for localized corrosion and, later on, film breakdown leading to actual pits or crevices at the micrometer scale [14].

The benefits of small amounts of Mo and W in combination with Cr in both Ni-based and Fe-based alloys have been known for some time and the existence of a Cr–Mo synergy in corrosion resistance is suggested based on empirical evidence [2]. Neither Ni-Mo nor Ni-Cr alloys achieve the beneficial combined impact that Cr and Mo impart when alloyed combination in acidic chloride solutions [22–25]. Much previous work posits that Mo is operative during the repassivation stage, while chromium is effective mainly towards passivation [12]. This view largely neglects the role of Mo or W in the passive film even though evidence of Mo benefits towards passivation is seen in Fe-Ni-Cr-Mo and Ni-Cr-Mo alloys [10,26]. To this end, the effect of Mo often concerns only repassivation and/or pit stabilization. However, another part of the research community has argued for many years that Mo operates with benefits towards both passivation and protective functions in the breakdown process, providing resistance towards trigger events which lead to local dissolution of the passivating layer [15,27–31]. It was also emphasized that highly corrosion resistant alloys in relatively benign environments suffer from pitting [21] due to the rate-controlling, localized, passive film breakdown, while less resistant alloys containing many defects and/or detrimental phases undergo many breakdown events and pit stabilization at readily formed initiation sites is the critical factor for attack severity.

The role of Mo in the pit stabilization and repassivation stages is well supported by experimental findings. However, increasing evidence supports the theory that aliovalent Mo cations present in the Cr-rich oxide play an important role towards both passivation and resisting passivation breakdown. This concept was formalized in the Solute-Vacancy Interaction Model [32]. Recently, this phenomena has been revisited and supported by the high likelihood that Mo is present in the form of individual cations in rapidly growing Ni^{2+} and Cr^{3+} oxide films due to a non-equilibrium solute capture phenomena [33]. Hence, solid solution oxides containing significant amounts of Mo and W solute as substitutional impurities at solvent cation sites in super-saturated concentrations are likely. In fact, the concentration of Mo and W cations in the oxide should be equivalent to the alloying composition in terms of cation percentage during rapid passivation and solute capture [33]. The question remains as to the exact functions of these minor alloying additions once they are found in a non-stoichiometric solid solution oxide.

Following a brief introduction to alloy classification and their fundamental corrosion performance, the current mechanistic understandings of Mo in each stage of a local corrosion process on a corrosion resistant alloy (CRA) is discussed. This discussion begins with thermodynamic predictions and experimental observations of the passive film composition for various alloys in selected environments, followed by a focus on the influence of minor alloying elements (e.g. Mo and W) on the oxide defect chemistry. Finally, the significant roles these additions play in preventing chloride-assisted breakdown by facilitating repassivation at local instabilities or incipient corrosion sites are introduced. It is worth noting that the effects bridge many length scales from subnanometer (atomic arrangements) to nanometers (thin oxides) and micrometers (crevice sites of attack).

2. Alloys and metallurgy

Ni-based alloys are ductile face-centered cubic (FCC) materials with high resistance to corrosive environments, high temperatures, and stresses. Moreover, they exhibit good creep resistance [1]. They are resistant to corrosion in fresh water, atmospheric conditions, and deaerated non-oxidizing acids, as well as in dilute caustics as covered in handbooks and commercial product literature [1]. Ni offers higher solubility for Cr and Mo, possessing attributes such as atomic radius and electronic configuration which enable a Ni solvent to accommodate substantial solutes without the formation of a second phase [1]. Due to this, alloys may be designed by adjusting major and minor additions for particular service environments and have even been optimized in some cases for service in both oxidizing and reducing acids [1,34,35].

Two families of alloys are often considered but the boundary between them is not sharp [1,7]. High temperature alloys usually contain concentrations of C and multiple phases which facilitate precipitation hardening. In contrast, solid solution alloys are typically intended for service in low temperature, aqueous environments and contain less C, which is detrimental towards corrosion behavior when carbides form.

Handbooks and commercial alloy literature document the propensity for various Ni-Cr-Mo-X (X = W, Nb, Ta, Fe, Cu) alloys to resist corrosion in various environments. Table 1 lists compositions for selected commercial alloys for which this review is relevant. A brief summary of alloying elements is warranted, given the strong role of certain alloying elements. Fe is usually added to facilitate less expensive incorporation of other elements [1,8]. Cr in particular is added to form passive films which resist hot gases and certain reducing and oxidizing acids. In chloride-containing environments, alloying with Cr improves passivity and inhibits breakdown. Cu is also alloyed to Ni-Cr-Mo-Fe alloys to inhibit localized dissolution in the presence of certain acids [1,8]. Mo and W enhance the film resistance to oxidizing and reducing acids and are especially useful in the case of chloride-induced pitting and crevice corrosion. Because of their high solubility, Cr, Mo, and W contribute some solid solution strengthening. Elements like Nb and Ti getter C, while elements such as Al contribute to strengthening mechanisms by age hardening. These alloys can be strengthened by cold work and precipitation age hardening at low temperatures through the

Table 1
Common commercial, low-temperature Ni-based alloys present in literature that are applicable to this review. Included are PREN values computed using Eq. (1).

Minor Alloying (Mo and W) of Ni-Based Alloys
Commercial Alloys

Alloy	UNS	Chemical Composition (wt.%)	PREN	Ref.
825	N08825	43Ni-21Cr-30Fe-3Mo-2.2Cu-1Ti	31	[10,45,49,50]
C-276	N10276	59Ni-16Cr-16Mo-4W-5Fe	71	
625	N06625	62Ni-21Cr-9Mo-3.7Nb	51	
C-22	N06200	59Ni-22Cr-13Mo-3W-3Fe	66	
C-2000	N06059	59Ni-23Cr-16Mo-1.6Cu	76	
59	N06059	59Ni-23Cr-16Mo-1Fe	76	
686	N06686	46Ni-21Cr-16Mo-4W-5Fe	76	
C-22HS	N07022	59Ni-21Cr-17Mo	77	
HYBRID-BC1	N10362	62Ni-22Mo-15Cr-2Fe-0.3Al	72	
600	N06600	72.87Ni-16.49Cr-9.46Fe-[CMnSiSCuNbTaTiAlCoP] < 0.4	16	

formation of coherent and semi-coherent Ni_3Al or Ni_3Ti phases known as gamma prime (γ') phases [1].

Ni-Cr-Mo alloys are often designed up to solubility limits at room temperature and a metastable solid solution exists below the solutionizing temperature (1150–1050 °C) after rapid quenching [36]. The metastable solid solution can be maintained for long times. Carbon is often minimized, with the formation of carbides or other phases on grain boundaries avoided using rapid quenching from the solutionizing temperatures and subsequent low temperature exposures below 427 °C [1]. Carbide precipitation and sensitization is not usually seen in modern Ni-Cr-Mo alloys. Extended aging above 427 °C causes long range ordering, forming topologically closed-packed phases. At higher temperatures above 593 °C, μ, σ, or P phases may form [10]. The transition temperatures reported depend on the exact Ni-Cr-Mo alloying content and the concentrations of C and Si, which are usually controlled [37–40]. Their formation of these secondary phases can be detrimental, especially when elements such as Mo and Cr have strong affinity and become depleted in the matrix.

The basis for ranking the corrosion resistance of corrosion resistant alloys (CRAs) such as those in Table 1 according to the beneficial effects of certain alloying additions is given by the pitting resistance equivalent number (PREN) (Eq. (1)). The empirical quantity is based on the weight percentages of Cr, Mo, and W where a higher PREN suggests better corrosion resistance. It is generally applicable to exposure of stainless steels and was later adapted for Ni-based alloys to gauge corrosion resistance in aqueous chloride environments [41]:

$$\text{PREN} = [\text{Cr}] + 3.3[\text{Mo}] + 0.5[\text{W}] \quad (1)$$

In a more qualitative form, the same trends captured in Eq. (1) are often reported. For instance, Mishra reports that resistance to local corrosion in hot chlorides for commercial off the shelf (COTS) alloys follows a systematic trend from least to most corrosion resistant: *high Cr - low Mo < low Cr - high Mo < high Cr – high Mo < high Cr – high (Mo + W)* [42].

The PREN concept has many shortcomings and underscores the needs, gaps, and opportunities with respect to understanding the function of minor element alloying highlighted herein. The ranking was empirically developed and although the benefit of elements in complex high entropy alloys (HEA) was recently forecasted [43,44], predictions outside of the database of Ni-Cr-Mo alloys given in Table 1 are uncertain. Moreover, the rankings of alloys may change for specific exposure environments [45] and the expression does not account for many of the other alloying elements possible. Microstructural effects such as crystal structure, second phases, grain size, and/or texture are also not considered [46–48]. The PREN does not delineate whether the alloying element effects operate during the passive film formation, breakdown, stabilization, or repassivation stages, nor the exact atomic mechanism. Finally, the PREN has no way to predict synergistically positive or negative combinations of alloying elements or to account for the Cr-Mo benefit in combination, nor the unique combination and complex interactions of multiple elements such as in an equiatomic or high entropy alloy [44]. New understandings of the atomistic role of individual alloying elements during electrochemical passivation, breakdown, and transpassivity are necessary to appropriately predict the corrosion behavior of an alloy or to computationally design one [14,30].

3. Basic electrochemical findings and observations

3.1. Passivation: E-Log (i) polarization behavior

The significant influence of minor alloying elements on passivity is often illustrated using E-log (i) polarization plots which report the relationship between the current density and applied potential [51]. The basic details of these diagrams and the implications for passivity are discussed elsewhere [2,26,51]. For passive materials, there is a

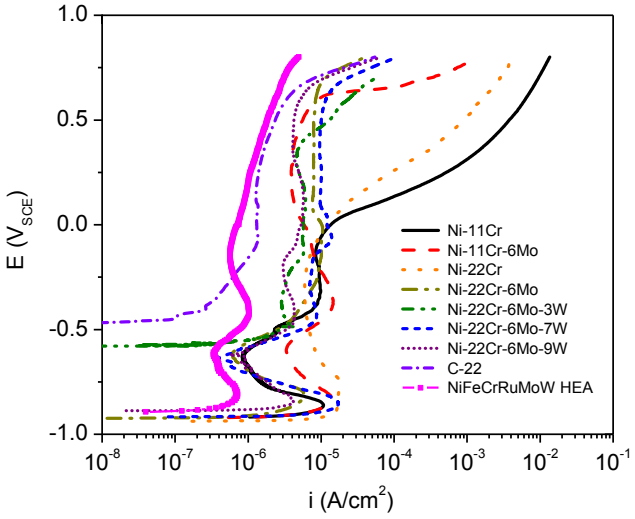

Fig. 1. Upward polarization curve of various Ni-based alloys, with their compositions given in wt%. Tests were performed in deaerated 0.1 M NaCl pH 4 with an upward scan rate of 1 mV/s from −100 mV vs OCP to +800 mV$_{SCE}$.

potential at which the metal-electrolyte interface begins to undergo an active to passive transition, E_{pp}, often occurring at a "nose" or peak in the current density. Following this potential, the measured current density decreases by several orders of magnitude before reaching a pseudo-constant value which corresponds to the corrosion rate of the alloy in the passive state, i_{pass}. Upon adding certain alloying elements such as Mo and increasing their concentrations, E_{pp} is typically shifted to more negative potentials and i_{pass} decreases significantly. This is evident in Fig. 1 where i_{pass} decreases as more Cr, Mo, and W are added to the alloys. The observed values of i_{pass}, however, also vary with [Cl^-] (Fig. 2). Notably, Ni-11% Cr has the highest i_{pass} due to the increase in Ni^{2+} cation vacancies upon solid solution substitution of Cr^{3+} in a NiO lattice. Further increases of Cr or Mo and W additions suppress i_{pass} by facilitating improved passivity due to (i) formation of continuous, stoichiometric oxide layers such as Cr_2O_3, (ii) doping with Mo^{n+} in a M^{m+} lattice (where n > m) and the possible inhibition of cation vacancy motion, and/or (iii) formation of a greater amount of corundum promoted by Mo and/or W alloying as will be discussed in greater detail below.

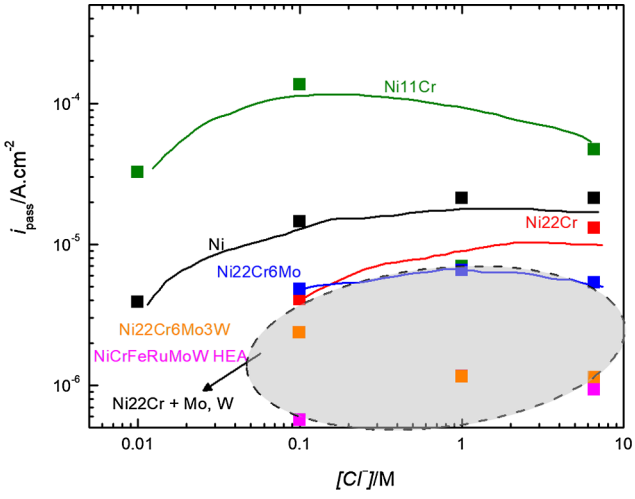

Fig. 2. Passive current density (i_{pass}) determined from polarization scans (e.g. Fig. 1) in various, deaerated pH 4 NaCl environments for several Ni-based alloys where the hashed region indicates the observed values of i_{pass} for Ni-Cr-(Mo + W) alloys in general.

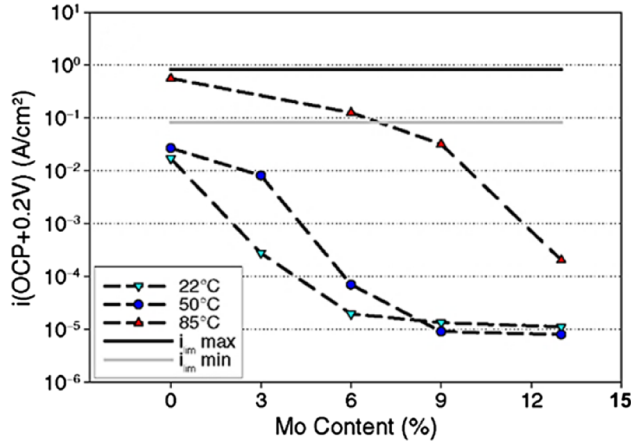

Fig. 3. Dependence of the anodic current density, i, at +200 mV_{OCP}, on the Mo content for Ni-22% Cr-X% Mo, wt%, model alloys. Tests were performed in deaerated 1 M HCl solution at 22, 50, and 85 °C with the calculated mass-transport-limited current density range, i_{lim}, shown for comparison. (Reproduced with permission from NACE International, Houston, TX. All rights reserved. [75]).

At increasing potentials, the passive films tend to break down due to either localized corrosion (e.g. crevice or pitting) or Cr^{3+}/Cr^{6+} transpassive dissolution [52–55] ($2Cr^{3+} + 7H_2O = Cr_2O_7^{2-} + 14H^+ + 6e^-$, $E(pH4) \approx +778mV_{SHE} = +534mV_{SCE}$) [56]. O_2 evolution is also possible at high electrode potentials. Supplementing the alloy with W further decreases the passive film dissolution rate at high potentials where Cr transpassivity is compensated by Mo and W oxide formation [12]. The most evidence of this effect is seen for the HEA in Fig. 1. Along with decreasing i_{pass}, increasing the Mo + W alloying element concentration in a metal will result in an increased breakdown potential for localized corrosion [41]. This effect becomes significant in more corrosive (i.e. acidic, chloride-rich, or high temperature) solutions. Fig. 3 demonstrates that even in an 85 °C solution where most alloys would experience fast, localized corrosion attack at +200 mV_{OCP}, increasing [Mo] results in a lower corrosion rate.

3.2. Potential step passivation

For alloys under a constant applied potential above E_{pp}, but below those where transpassive or localized corrosion would occur, the thickness of a passive film increases with time [57]. The kinetics of this phenomenon have been the subject of several oxidation models [58–65]. At long passivation times in aqueous environments, a quasi-steady state or limiting thickness is typically reached where the continual residual rate of oxidation at the metal/oxide interface becomes equivalent to that of oxide dissolution, whether oxidative or chemical, at the oxide/electrolyte interface [66]. Both the chemical dissolution and chloride-induced breakdown of passive films can be similarly modeled through application of various rate equations that vary from one model to the other [27,67,68]. Additionally, the initiation and propagation of pitting on the surface of oxides has been the subject of modeling efforts [21,27,69–71]. For the case of Ni-based alloys, it has been seen that increasing the applied potential results in a pseudo-linear increase in steady state film thickness up until chemical dissolution causes linear thinning [12,72]. Similarly, increasing the alloying ratio of Cr:Mo results in thicker films at a given potential [12]. It was also found that the presence of W in C-276 and C-22 further increased the film thickness compared to C-2000, which possesses a similar Cr and Mo content [12].

Several recent studies have investigated the influence of crystallographic orientation on the competition between passivation and chemical dissolution for Ni-based alloys [46,47]. Through the application of single frequency electrochemical impedance spectroscopy and atomic force microscopy, a greater propensity for conformal film formation was seen on low index grain orientations close to (1 0 1) for a Ni-11%Cr alloy, The test was conducted in an acidic NaCl solution during potential controlled passivation. In the case of Ni-11%Cr-6%Mo, repassivation was observed at all orientations under potential control [46]. For a more corrosion resistant alloy, C-22, it has been shown however that greater dissolution occurs for (1 1 0) grains during etching in 3 M HCl where the metal surface likely has no protective oxide, with (1 1 1) exhibiting the least damage [47]. However, upon etching the surfaces in 1 M HCl where an oxide film was stable, the (1 1 0) oriented grains were observed to have a lower corrosion rate due to stability of a favorable oxide and the decreased likelihood of chloride-assisted film breakdown [47].

Pitting and crevice corrosion, especially stabilization and propagation can be inhibited by alloying with Mo and W because of both lower active dissolution rates and a greater propensity for the film to repassivate [2,73–75]. The exact mechanism by which this occurs is not fully understood, but there are multiple theories that will be discussed below. In general, however, the induction time for pitting or crevice corrosion events will increase with the combination of higher Cr + Mo + W alloying content. Figs. 4 and 5 demonstrates this, where Ni-11% Cr and Ni-11%Cr-6%Mo crevice corrode after only approximately 200–300 s, whereas Ni-22% Cr and Ni-22% Cr-6% Mo remain passive for thousands of seconds and exhibit lower propagation rates if breakdown occurs. The W-containing alloy (Fig. 5), however, remained passive for the entire, albeit relatively short, measurement time. Fig. 5 focuses on exclusively the alloys with 22% Cr and Mo or Mo + W. Passive current densities are lower and fewer metastable breakdown events are evident. The crevice corrosion initiation behavior trends in commercial alloys listed in Table 1 are given in Fig. 6.

3.3. Metastable pitting of alloys with protective passive films

In environments where Ni-based alloys are protected by passive films, minor alloying elements often increase the film breakdown potential as discussed in Section 3.2. There is an impact on breakdown initiation at potentials within the passive region where metastable pitting is likely, but delayed initiation and fast repassivation is facilitated by Mo or W alloying additions in alloys with sufficient Cr.

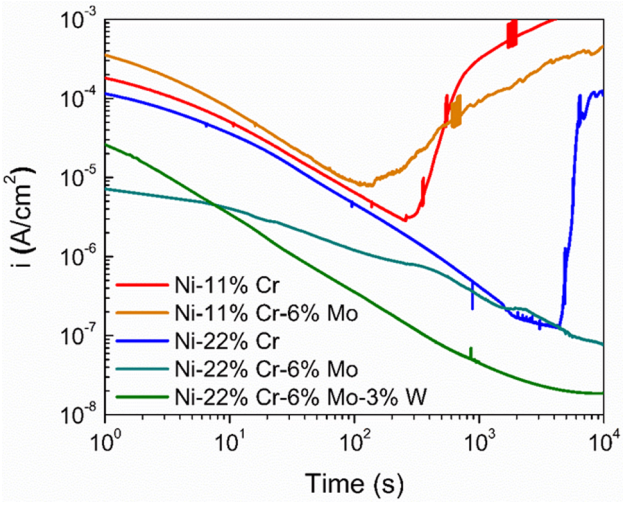

Fig. 4. Current measured during potentiostatic potential–step passivation at +200 mV_{SCE} for various Ni-based alloys (wt%) in deaerated 0.1 M NaCl pH 4, where the initial current decay indicates film growth. The low [Cr + Mo + W] alloys exhibited abrupt current increases at shorter times, indicative of decreased resistance to localized pitting or crevice corrosion.

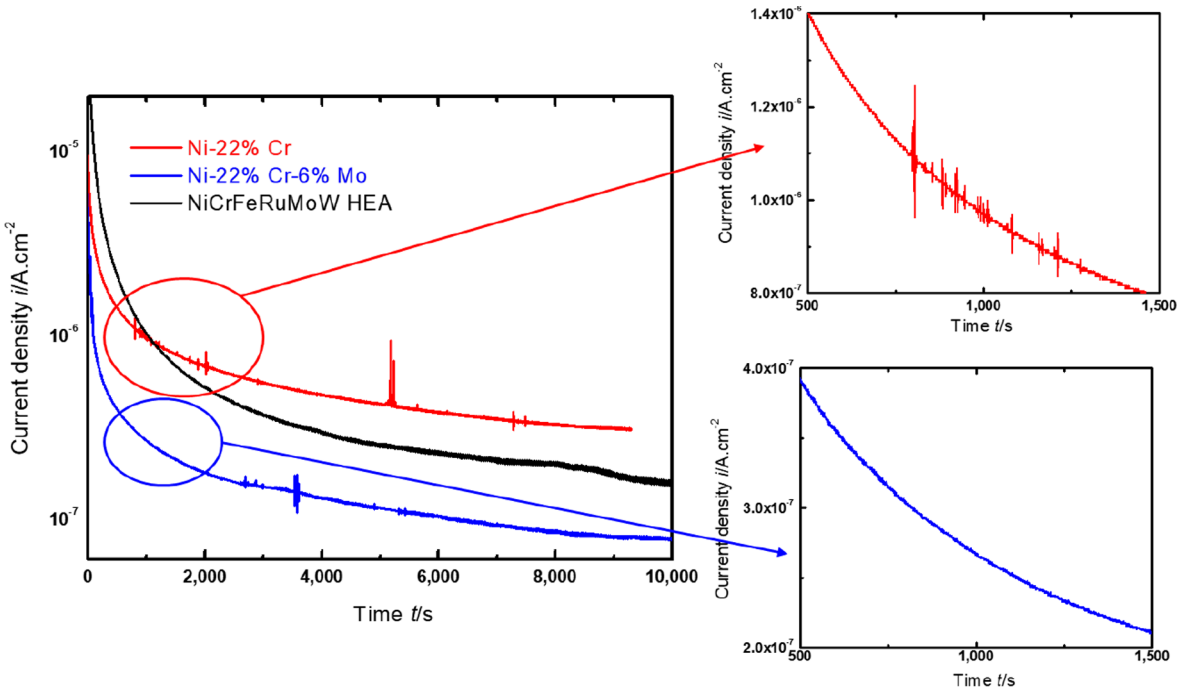

Fig. 5. Metastable breakdown of the films grown on Ni-22% Cr and Ni-22% Cr-6% Mo, wt%, during potentiostatic passivation at +200 mV_{SCE} and on the NiCrFeRuMoW HEA (Table 1) at +300 mV_{SCE} in deaerated 0.1 M NaCl pH 4.

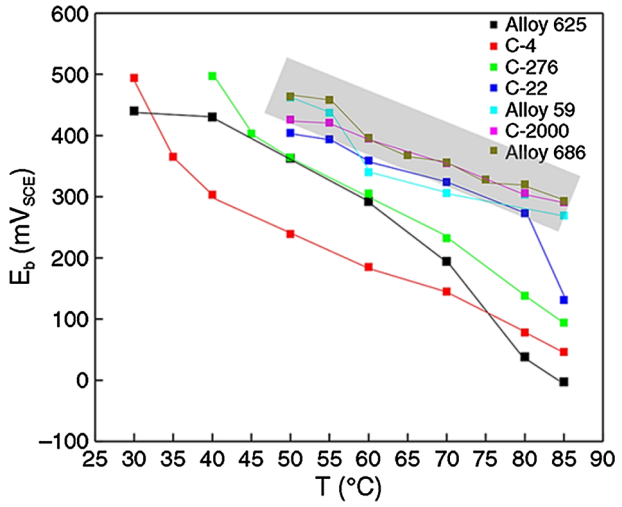

Fig. 6. Breakdown potentials, E_b, for various commercial Ni-Cr-Mo-W alloys determined as a function of solution temperature. E_b was determined using galvanostatic polarization for times up to 40 hr in 1 M NaCl solution at the temperature indicated. The shaded region corresponds to alloys with both high Cr and high Mo + W content (Table 1). (Reproduced with permission from NACE International, Houston, TX. All rights reserved. [41]).

These alloys only undergo metastable breakdown, followed by rapid repassivation [76]. This behavior is commonly observed on stainless steels and Ni-based alloys [77–81]. The measured anodic passive current will decay as the film thickness increases under potentiostatic conditions, [58]. Metastable breakdown, however, results in current spikes due to the contribution of fast, transient dissolution as shown in Fig. 5. Adding minor alloying elements can, as such, decrease the frequency and induction time for these events [27]. This behavior is shown in Fig. 5, where the Mo-containing alloy experienced no discernable metastable pitting at early times. Even at longer times, fewer current spikes were measured for this alloy compared to Ni-Cr. Upon the additional alloying of Fe, Ru, and W into HEA, no metastable activity was recorded during 10 ks of passivation at +0.3 V_{SCE} despite the increased potential.

3.4. Stable breakdown and threshold potentials for local corrosion

At any given temperature, the alloys corresponding to both high-Cr and high Mo + W content exhibited greater breakdown potentials than the others in NaCl solutions [41]. In addition, these heavily alloyed Ni-based materials did not exhibit breakdown and crevice corrosion for the entire 40 hr exposure period at solution temperatures below 50 °C.

The results in Sections 3.1–3.4 collectively underscore the benefits of Cr combined with Mo + W (i.e., a high PREN) in stages ranging from passivation to stable breakdown and local corrosion. However, only vague information regarding the benefit of a high PREN on the different stages of corrosion can be discerned. Moreover, there is limited information at various length and time scales governing attack and limited information concerning the exact mechanism [14,82].

4. Thermodynamic predictors of passivity: pourbaix E-pH and speciation diagrams

Given the strong effects of alloying on Ni-Cr alloys, the first aspect to examine is thermodynamic predictors of protective passivation. The electrochemical stability of a passive film in aqueous environments is often directly tied to its thermodynamic stability. By inspecting the standard Gibbs formation energy, ΔG_f^o, for individual oxide or hydroxide species that can be formed, the most thermodynamically stable compound can be ascertained. The computed ΔG_f^o values can then be converted into chemical potentials and for a given electrochemical reaction, the corresponding Nernst equilibrium potential [56]. In the case of multi-element alloys, a stable, stoichiometric oxide species for each metal component is predicted to contribute towards film growth. For example, when Ni passivates, it typically forms NiO ($\Delta G_f^o \approx -215\ \frac{kJ}{mol}$), and/or $Ni(OH)_2$ in a state of hydration [56,66,83]. While the most thermodynamically-stable oxide might form, there are other situations in which the kinetically-favorable oxide will instead be favored [33,66]. For Ni-Cr alloys, the most stable stoichiometric species are often Cr-rich

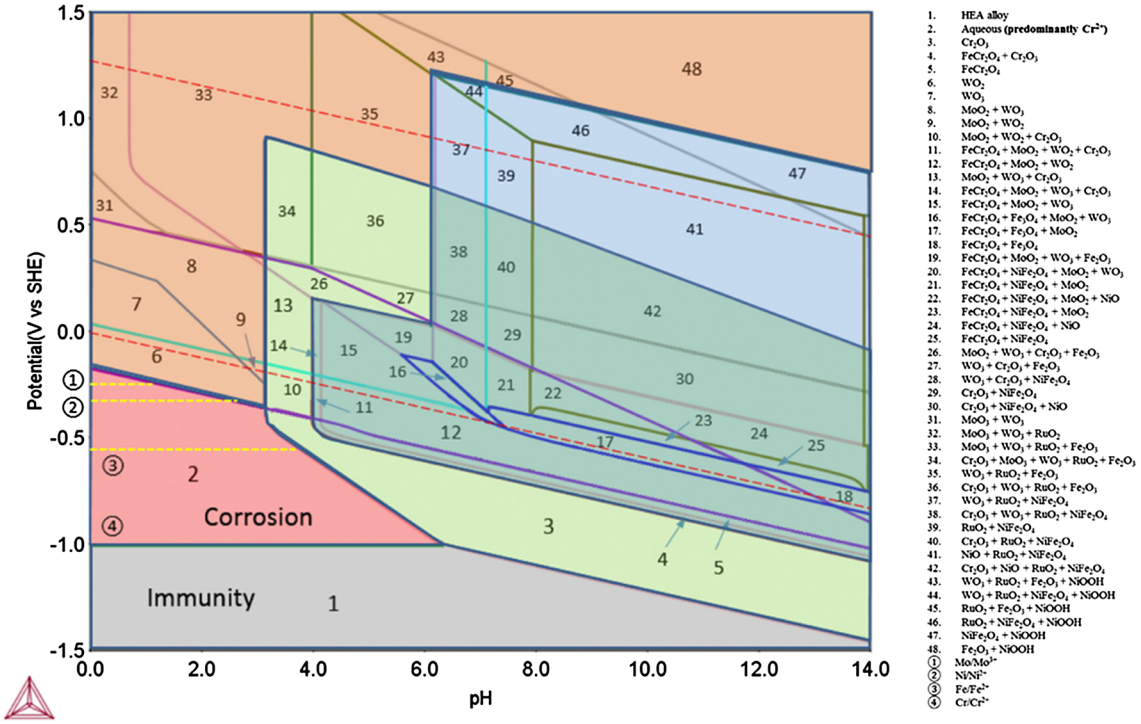

Fig. 7. CALPHAD-calculated E-pH diagram for $Ni_{38}Cr_{21}Fe_{20}Ru_{13}Mo_6W_2$ in 1 kg H_2O at 25 °C and 1 atm. The red dashed lines are reversible potentials for hydrogen and oxygen evolutions, and the yellow dashed lines are the metal/aqueous ion equilibrium lines for pure constituent elements. The red region indicates where oxidized aqueous species are stable, green where Cr_2O_3 is stable, blue where Fe-Ni, Fe-Cr spinels are stable with some overlap with the green, and orange where oxides are stable. Only stoichiometric oxides are considered. (Reprinted from [44] with permission from Elsevier.) (For interpretation of the references to colour in this figure legend, the reader is referred to the web version of this article.)

(e.g. $\Delta G^o_{fCr_2O_3} = -1,058\ \frac{kJ}{mol}$ and $\Delta G^o_{fNiCr_2O_4} = -1,257\ \frac{kJ}{mol}$) [84]. In alloys containing sufficient Fe alloying, various spinels species with favorable stability can be formed (i.e. $NiFe_2O_4$ and $FeCr_2O_4$). Hence, thermodynamics support the notion that dominant oxides should be corundum and various spinels.

The thermodynamic stability of pure metals and alloys at varying electrochemical potentials and pH's are portrayed in Pourbaix E-pH diagrams [44,56]. Typically, diagrams are constructed at 10^{-4} or 10^{-6} M cation concentrations, but near-saturated concentrations may exist in confined spaces such as crevices [44]. These diagrams historically exist for thermodynamic equilibrium mainly for single elements not alloys, do not consider the effects of adsorbed species and epitaxy on oxide stability or kinetic effects [85]. At sufficiently negative potentials, metallic elements are typically stable for all pH with regions at greater potentials indicating passivation and corrosion. Through overlaying the chemical equilibrium Pourbaix diagrams for each element present in an alloy, the general stability of an alloy can be inferred. Today, an improved approach is to compute a phase diagram for multi-component solid solution alloys. In this case, single and binary element oxides and hydroxides are often considered [44,86,87]. Most diagrams do not consider oxides or hydroxides involving multiple alloying elements. Commercial software such as CALPHAD, MEDUSA or OLI[1] are capable of calculating the E-pH diagrams by predicting where alloys will form stable oxides of the limited types mentioned in a given environment for various applied conditions. Fig. 7 indicates such a diagram for a $Ni_{38}Cr_{21}Fe_{20}Ru_{13}Mo_6W_2$ HEA [44]. Overall stability is predicted outside the red area at low pH indicative of strong reducing acids where most oxides chemically dissolve. Stability elsewhere owes to the presence of one or more thermodynamically stable oxides. Stoichiometric oxides and/or spinels of at least one element are thermodynamically stable at each E-pH condition indicated by the green, blue, and peach regions. However, the diagram does not indicate whether a critical threshold alloying content exists to produce a coverage nor can it handle kinetically controlled enrichment. Moreover, in many practical applications, observed passivity extends past what is predicted by Pourbaix diagrams due to the existence of metastable films which are kinetically enabled due to a balance between fast, metastable film formation and slower chemical dissolution. As such, Cr-rich films are often observed to remain passive at pH 3 and below while not predicted at thermodynamic equilibrium [12,44,88–90].

5. Observed passive film compositions and the fate of minor alloying elements

While in general the empirical corrosion properties of Ni-alloys, especially common commercial ones like C-22, are well-established [50,89–92], a full understanding of the exact atomic mechanism by which specific alloying elements act has not been achieved [30]. The results are mainly empirical with some insight through work on nuclear waste repository container work on commercial alloys [12,17,72,91,93,94]. Similar to stainless steels, increasing [Cr] in a Ni-Cr alloy will result in a decrease of the corrosion rate in reducing acid, neutral, and chloride solutions [2]. Likewise, alloying of Mo and W promotes a similar decrease in the measured uniform passive corrosion rate of Fe-Cr and Ni-Cr-based alloys [95]. The corrosion rate drops significantly, however, when a critical concentration of Cr is reached (i.e. > 12 wt% Cr in Fe, > 8–11 wt% Cr in Ni) and a uniform, Cr-rich, passive film layer (often assumed to be Cr_2O_3 or $Cr(OH)_3$) forms across the oxide surface [12,24,96,97]. The origin of the threshold is debated today and various theories have been posited such as graph theory, bond percolation, and kinetically controlled enrichment governed by dissimilar dissolution rates of alloying elements [12,17,24,25,96–99]. The cation fractions seen in these alloys have been studied by XPS. The

[1] These products can be accessed at the following sites: calphad.org, kth.se/che/medusa/chemeq-1.369367, and olisystems.com/

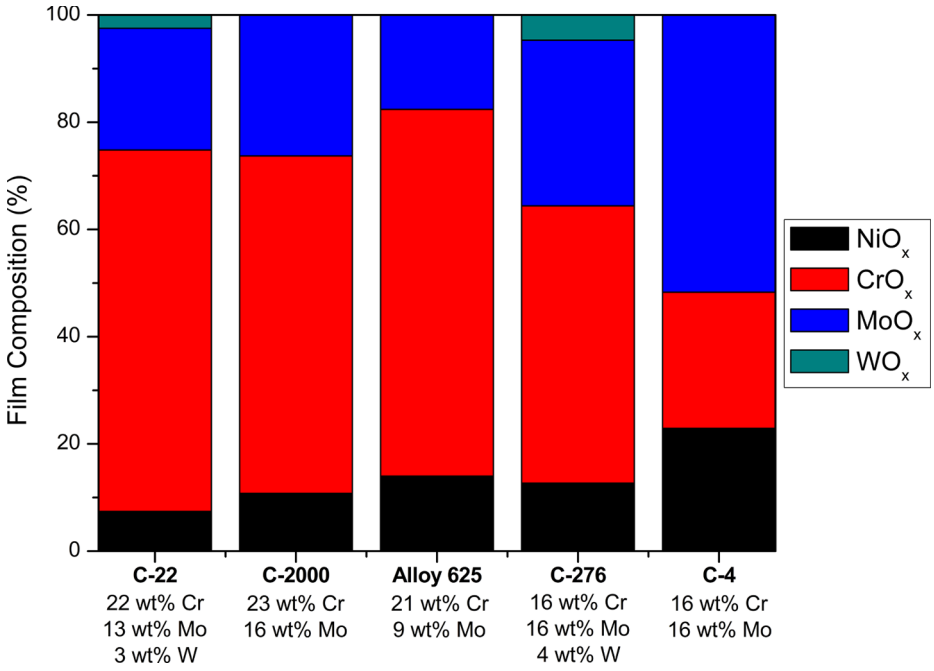

Fig. 8. Passive film composition of various commercial Ni-alloys as measured using XPS following passivation at +305 mV_{SCE} for 3 d in aqueous 1.0 M NaCl pH 0 solution heated to 75 °C. (Reprinted from [17] with permission from Elsevier.)

result of preferential oxidation of Cr over Ni is shown in Fig. 8. It should be noted that there is a decreasing molecular fraction of Ni-rich oxides detected compared to Cr^{3+} as [Mo + W] alloying content is increased such as in the case of C-22, C-2000, and Alloy 625. This effect is especially evident in alloys containing W, as indicated for C-22. Notably, these alloys have an approximately constant bulk Cr composition [17]. While the primary role of Cr in enabling passive film stability is understood, the additional complexion of minor alloying elements and their function regarding the growth mechanism, composition, and structure of passive films formed in electrochemical environments remains less certain [30,100,101]. The synergistic interactions of Mo and W within Cr-rich passive films and the overall increases in the localized corrosion resistance are commonly observed as reviewed above in 3.1–3.4 [9,17,32,102,103], but the effect otherwise remains unclear and controversial [32,104]. Thus, the possible beneficial effects of other oxide dopants introduced as alloying elements cannot be predicted. Because of this alloy design continues to evolve according to trial and error rather than scientific understanding.

The majority of relevant literature concerns the constant-potential passivation of Ni-based superalloys, such as C-22, in moderately concentrated NaCl solutions. Layered, phase-separated, stoichiometric oxides were generally assumed: a Cr_2O_3 or $Cr(OH)_3$-rich film present at the inner interface and a NiO or $Ni(OH)_2$ outer film [92,105,106], with preferential accumulation of Mo^{6+} and/or Mo^{5+} cations at the oxide/electrolyte interface. It has been found that, in general, Cr and Mo preferentially segregate to the metal/film and film/electrolyte interfaces, respectively [107]. This analysis might be flawed as it is based on the XPS binding energies for $Mo^{4,5,6+}$, Cr^{3+} and Ni^{2+} as seen in MoO_x, CrO_x, and NiO_x layers [12,108], but chemical characterization alone does not provide structural information regarding the oxide identity and thus cannot prove that these distinct, phase-separated, and pure stoichiometric oxides exist. More recent work utilizing 3D atom probe tomography (3DAPT) has observed a similar distribution of elements throughout the film. However, these studies report non-stoichiometric oxides, rationalized by the occurrence of nonequilibrium solute capture [33]. At room temperature these oxides are solid solutions which do not exhibit distinct, phase-separated reactive layers. High entropy alloys also have been observed to form complex non-stoichiometric oxides [43].

In contrast, distinct phases form at high temperature where equilibrium conditions are often reached. *In operando* transmission electron microscopy (TEM) was also applied to understand the early stages of film growth on Ni-Cr alloys at 700 °C [109,110]. In these studies, the initial oxidation of dilute Ni-10 at% Cr was revealed to proceed by surface diffusion of Ni and O atoms, followed by the nucleation of subsurface Cr_2O_3 [109]. $NiCr_2O_4$ islands were nucleated, but it was observed that secondary NiO "whisker" phases grew out of the oxide plane and resulted in uneven layering of the different compounds. For the case of Ni-20 at% Cr, subsurface Cr_2O_3 nuclei coalesced and large $NiCr_2O_4$ islands emerged from the NiO layer [110].

The influence of minor alloying elements on the chemical identity of passive films grown slowly on Ni-Cr-based alloys by high temperature oxidation [109–112] or electrochemical potentiostatic or open circuit potentials [12,17,93,106] has been well-addressed. Recently [113], it was also found that Ni-Cr-Mo alloys exhibit an epitaxial rock-salt oxide containing Ni, Cr and Mo in the rock salt structure during early stages of oxidation and later indicated corundum structures containing all alloying elements. Moreover, there were no Kirkendall voids found during *in operando* TEM experiments in Mo-containing oxides, suggesting a role for Mo dopants in inhibiting vacancy coalescence into voids in addition to preferentially oxidizing Cr^{3+}. In comparison, the rock-salt-structured oxide formed on Ni-Cr contained Kirkendall voids, as shown in Fig. 9b. These results are, however, only indicative of film growth under dry oxidation conditions. There will be a significant influence of aqueous dissolution on both nucleation and growth of oxides in electrochemical environments and thus the mechanism of the oxidation process will likely adjust [66]. Water enhances passivity via dissociation into protons which can occupy interstitial lattice positions in the oxide, consequently lowering the vacancy formation energy and the diffusion barrier for both cations and anions [114]. As a result, faster oxidation kinetics should occur in aqueous solutions.

The quantitative effects of alloying Fe with Cr, Ni, Mo, and W on passivation kinetics have also been extensively studied and it was found that both the passivation rate and film stability increased with the concentration of minor elements [115,116]. Kinetic analysis of oxidation through the application of the Cabrera-Mott model to repassivation phenomena has similarly shown that Mo and W facilitate more facile

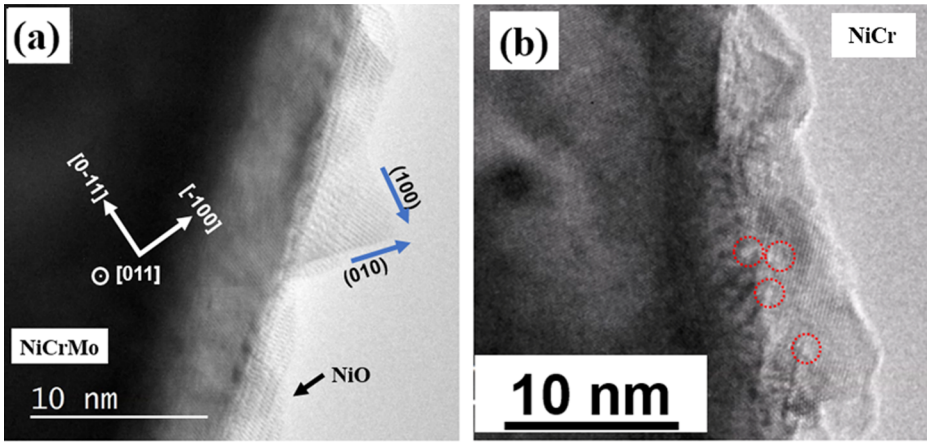

Fig. 9. (a) *In situ* TEM images of initial layer-by-layer growth of NiO on Ni-Cr-Mo surfaces in O2 where the NiO island has {1 0 0} surfaces and the blue arrows show the layer-by-layer growth direction. For comparison, (b) presents *in situ* TEM images showing Kirkendall voids (dotted circles) formed near the oxide-metal interface of the Ni-Cr alloy. (Reproduced with permission from NACE International, Houston, TX. All rights reserved. [113]). (For interpretation of the references to colour in this figure legend, the reader is referred to the web version of this article.)

scratch-repassivation and therefore decrease the stress corrosion cracking susceptibility [95]. Similarly, the influences of these alloying additions on high temperature oxidation were found to be similar, where Cr cation transport controls scale growth [111] and Mo impacts growth by increasing the passivation rate and preventing the formation of Kirkendall voids at the metal/scale interface, presumably through electrostatically interacting with metal cation vacancies and reducing their mobility [117].

Recent modeling work has also demonstrated the beneficial impact of Mo alloying on O adsorption on Ni (1 1 1) and Ni-Cr (1 1 1) surfaces [118]. These recent first-principles models showed that O adsorption was thermodynamically favorable at sites adjacent to Cr and Mo atoms (Fig. 10). Moreover, a significant influence of Mo is seen when O is bonded to Ni and/or Mo atoms as it stabilizes the oxidation reaction by donating more charge than either Ni or Cr. While this model is simplistic considering a perfect Ni-Cr surface, the observation that Mo facilitates oxygen adsorption and subsequent passivation of the metal surface for various configurations of the atoms contributes to the understanding of passivity of Ni-Cr-Mo alloys.

6. Defect chemistry with minor alloying additions

In this review, it has been established that solute capture leads to the trapping of large dopant concentrations in passive films. Ni typically exists as a charged metal cation (Ni^{2+}), Cr as Cr^{3+}, Mo as $Mo^{4,5,6+}$, and W as $W^{4,6+}$ [12]. The roles of specifically Mo during the atomic-scale physical, chemical, and electronic processes relevant for

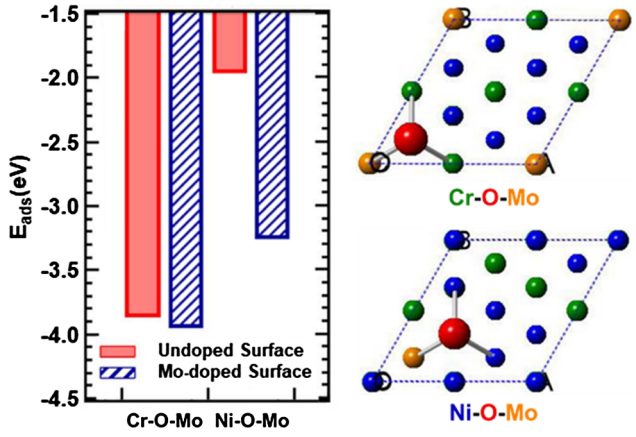

Fig. 10. Comparison of the FCC-site oxygen adsorption energy at 0.25 ML for the cases of the (1 1 1) alloy surfaces directly cut from the bulk and Mo-doped alloy surfaces with the relevant doped cases shown on the right. (Reprinted from [118] with permission from Elsevier.)

passive film growth have been theorized [15,29,32,105,117,119,120] and several models exist. Heretofore, these models are unproven because of two aspects: there has been no explanation for how the dopants arrived in the oxide nor quantitative proof of the theorized functions. It has been observed in previous literature that solute can be captured into a crystal structure during growth (i.e. Cr^{3+} present on a Ni^{2+} site in NiO), resulting in chemical doping of the passive film which was formerly only considered within typical oxide solubility limits but now has been shown to extend well beyond equilibrium stability levels [32,33,111,121,122]. For the situation where Mo^{6+} is substituted onto a Ni^{2+} or Cr^{3+} lattice site, the net positive charge results in the annihilation of electron holes and attraction of negatively charged defects, such as metal cation vacancies formed possibly by halide anion adsorption [27,32,61,123]. The resulting complex is neutrally charged and will not contribute towards growth of cation vacancy condensates, which the Point Defect Model (PDM) proposes are precursors for pit formation [27]. The generic reaction for this substitutional effect of Mo^{m+} into a M^{n+} cation site where m > n is given as [32]:

$$\left(\frac{n}{m-n}\right)Mo_M^{(m-n)\cdot} + V_M^{n'} = \left[\left(\frac{n}{m-n}\right)Mo_M^{(m-n)\cdot} \times V_M^{n'}\right]$$

This suggested influence of alloying additions such as Mo among other high cation valency elements on point defect transport across passive films corresponds well with previous work concerning the inhibition of the earliest stages of crevice corrosion on commercial Ni-based superalloys where the effect was largely brought about using low concentrations of dopants [20,75,81,124]. The effect of Mo on vacancy mobility has been additionally observed in the case of high temperature oxidation, where the alloying of small (< 1%) concentrations reduced the formation of Kirkendall voids at the metal/oxide interface [117]. An example of this significant impact on void formation is shown in Fig. 11.

The effect of W is similar to that of Mo as it tends to exist at the same cation valency when solute captured as dopants. In most Ni-based alloys, it is alloyed in tandem with Mo in order to optimize both the strength and corrosion properties, such that its individual impact cannot usually be ascertained [41,125]. A direct comparison can be made, however, through comparing a Ni-Cr-Mo (e.g. C-4) to a Ni-Cr-Mo-W alloy (e.g. C-276) where both have the same Cr and Mo concentrations. It has been previously shown that for these two commercial alloys, C-276 possesses a thicker passive film, greater Cr-film enrichment, and a lower corrosion rate in reducing acid environments [17]. The increase in film thickness upon adding Mo and/or W is often thought to be a result of their enrichment near the oxide/solution interface [92,102]. W-enriched oxides, however, have a solubility in acidic solutions 2 to 3 orders of magnitude lower than that of Mo-rich oxides, suggesting that the steady state dissolution rate of Ni-Cr-W would be slower for an equivalent Ni-Cr-Mo alloy [12,126,127]. W is,

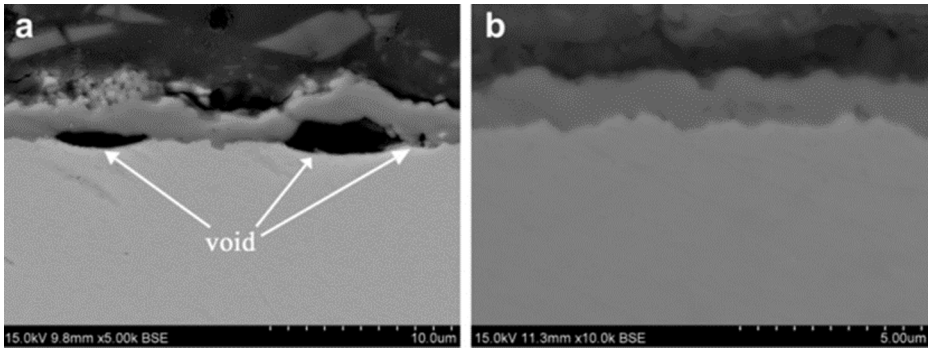

Fig. 11. Cross-sectional SEM images of the ferritic stainless steels after 500 h oxidation at 800 °C in air: (a) Fe-22%Cr-0.5%Mn and (b) Fe-22%Cr-0.5%Mn-0.1%Mo (wt%) showing voids. (Reprinted from [117] with permission from Elsevier.)

however, less soluble at equilibrium in Ni or Cr-enriched films and constitutes only up to 1 at% in passive films measured on various commercial alloys, whereas the concentration of Mo cations can range from 1 to 20 at% [12]. At minimum these elements can be solute captured in oxide films possibly in higher concentrations.

7. Theories of local corrosion mitigation

7.1. Effects of chloride adsorption, instabilities, and film breakdown

Chloride environments are well-known to complicate passivation reactions through chemical dissolution across the film layer [45,74,80,90,128–133]. In addition, chloride may lower the film surface energy and subsequently instabilities may trigger an abrupt breakdown event [128]. The influence of chloride on the breakdown of oxidized Ni (1 1 1) surfaces has been methodically studied through experiments and density functional theory (DFT) simulations [128,132,134–136]. On a defect-free NiO (1 1 1) surface, it was found that the chloride anions substitute hydroxyl groups via an exothermic reaction and this adsorption not only promotes greater surface coverage of Cl^-, but also induces local thinning of the passive film as chloride-containing compounds (i.e. Ni(OH)Cl or $NiCl_2$) were observed to detach from step edges [132]. However, $MoCl_x$ formation was presumed to be insignificant compared to $NiCl_2$ or $CrCl_3$ due to low formation free energies compared to the more favorable energies of various oxide species [87]. Sub-surface penetration of chloride can be achieved but is unlikely for undefective terraces in the passive film due to steric hindrances. The presence of defects in the film would only mediate halide anion adsorption and subsurface penetration. This is evident for preferential depassivation at grain boundaries, for example [74].

Adsorption of chloride becomes further complicated upon the introduction of multi-element alloys. Dissolution of individual minor alloying elements during passive film growth can result in a modification of the oxide chemistry [27,137]. In addition, chloride anion attack at the film/solution interface results in the formation of metal cation vacancies which can aggregate and form Kirkendall voids at the metal/film interface, shown schematically in Fig. 12 [74]. These clusters may cause instabilities and induce mechanical stresses in the film which, upon reaching a critical size, can rupture and form a corrosion pit. As mentioned previously, the addition of minor alloying elements such as Mo can inhibit the mobility of metal cation vacancies and, therefore, help prevent the formation of Kirkendall voids [137].

Additions of other minor alloying elements, such as Mo and W, can further impact growth by interacting with the other metals and/or electrolyte to promote variations in the film electronic or chemical properties. Their influence has been addressed with regards to the inhibition of localized corrosion events, but rarely during the passivation of alloys and before breakdown initiates. Even the effect of Mo on oxygen versus chloride adsorption mitigates the latter's effect on reducing the oxide surface energy [87]. Overall, the influences of Mo and W during film growth are particularly complicated, as previously mentioned, and are theorized to have crucial importance on film stability during passivation in chloride by modifying the kinetics of various point defect reactions [12,137]. This aspect of these alloying elements is largely open and underestimated.

7.2. Stabilization and repassivation of local corrosion sites

Local corrosion stabilization models of Ni-Cr-Mo alloys have previously involved a combination of the activation for a passive material which possesses or develops an active-passive transition, critical occluded solution chemistry, and, in the case of seawater crevice corrosion, dissolution-hydrolysis-acidification chloride migration [138–140]. These are also consistent with models which propose $E_{ocp} < E_{crit}$ for passivation because the IR drop from the mouth of the crevice to the crevice corrosion site places the potential in the nose of the active passive transition, especially when local sporadic breakdown occurs [81]. In the case of Ni-Cr-Mo alloys, the critical chemistry change model accounts for the development of the active region in an acidified crevice at high $[Cl^-]$. In order to stabilize the crevice site against repassivation, the crevice growth rate equals or exceeds the dissolution rate from the crevice. A salt film may aid this process by buffering the local pH to maintain the chemistry [21,69]. These theories by themselves do not predict, however, the role of minor alloying additions but provide a framework for examining various possible effects.

Steigerwald, Lizlovs, and Bond first showed the effect of Mo on the active passive transition in Fe-Ni-Cr alloys [141]. Later, Newman showed that active dissolution in artificial pits lowered the active kinetics of Fe-Cr-Mo alloy dissolution [142]. Bocher then showed the same effect in Ni-Cr-Mo alloys in strong HCl solution [75]. Raman spectroscopy has demonstrated this occurs by the formation of polymeric Mo and W species at active sites [72,143]. As more Mo and W were alloyed, the depth of attack was lower for Ni-Cr-Mo alloys with less [Mo + W] and the attack tends to spread out, suggesting initiation is not mitigated to the same extent by which propagation is hindered [81]. Further evidence of this was seen for an alloy containing 15% Cr and 22% Mo (HYBRID BC 1). Both the passive current density and repassivation potential were more favorable for these alloys compared to ones with less Mo and more Cr [144].

In light of this, the various roles of Mo in these various processes or stages of local corrosion may be reviewed. First, W and Mo form thermodynamically stable oxides at acidic pH levels unlike Cr and Ni. Moreover, the free energy of formation for $MoCl_3$ does not suggest its formation compared to Mo oxides [87]. Anderko described the solution chemistry of Mo in acidified chloride solutions and found stable MoO_2 and MoO_3 at low pH [142,145,146]. Hence, Mo can help Ni-Cr-Mo alloys resist formation of the critical chemistry and thus the development of an active/passive nose. Surface segregated Mo affects active

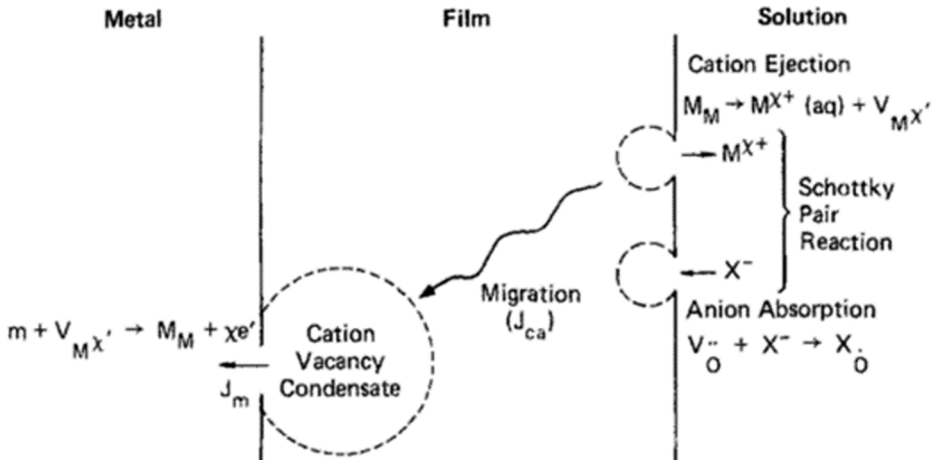

Fig. 12. Proposed processes leading to the breakdown of passive films according to the Point Defect Model. (Reprinted from [32] with permission from Elsevier.)

dissolution and both changes the crevice repassivation potential and alters the active passive transition. Mo has beneficial and detrimental effects in the solution phase at local corrosion sites. Mo dissolution may also form MoO_4^{2-} species which have been observed to lower pit or crevice dissolution rates by inhibiting the anodic reaction [9]. Jakupi furthered the work of these investigators by showing that Mo and W enriched on surfaces and corresponding polymeric species were observed in crevices via Raman spectroscopy and atomic emission spectroelectrochemistry [99,143]. Recently, the role of specifically Mo in enabling repassivation was attributed to the dynamic precipitation and dissolution of Mo in the local, acidic pit environments [99]. It is clear that Mo and W affect the initiation and stabilization stages of local corrosion sites as well as passive film growth in a variety of ways. A summary of all the possible benefits covered in this review is given here where Mo (and W):

1. Promote stronger O^{2-} adsorption [87,118]
2. Decrease favorability for Cl^- adsorption which, in turn, thwarts decreases in oxide surface energy [77,87,128]
3. Enable film enrichment of Cr^{3+} to higher cation fractions than seen in alloys without Mo or W at the same Cr content [12,17,106]
4. Bring about doping of $Mo^{4,5,6+}$ in oxide films that interact with point defects [32].
5. Produce favorable bonding to cation vacancies, enabling their subsequent immobilization [113,117]
6. Encourage precipitation of surface Mo-species in local acidic environments during transpassive dissolution and crevice corrosion [99,143]

8. Summary and future prospects

Mo and W are shown herein to operate in a number of ways to affect the corrosion resistance of Ni-based alloys containing Cr in a variety of stages of corrosion. There is no single mechanism that is solely operative as Mo and W function in a number of ways. There are more than one stage in which Mo and W operate. Mo and W impurities in a Ni-Cr surface favor oxygen chemisorption over binary Ni-Cr alloys on most surface oxide sites and may form oxides such as MoO_2 and MoO_3 in the outer layer of mature passive films [93]. Otherwise, Mo and W likely become trapped as substitutional $Mo^{4,5,6+}$ and W^{6+} cations in Ni^{2+} and Cr^{3+} oxides which may interact with negatively charged cation vacancies to reduce their mobility by electrostatic interactions. As a result, the formation of pits or crevices via vacancy clustering can be inhibited. Previous speculations have this been placed on firmer ground concerning the viability of this theory. Mo (and W) form strong bonds with adsorbed oxygen a first step during passivation. Finally, Mo and W also affect local corrosion site stabilization and repassivation by enriching at local corrosion sites, forming inhibitor phases, and restricting kinetics of dissolution. The presented results may have broader impacts than for Ni-Cr-Mo-W alloys alone. These fundamental unit processes can be manipulated in other material systems using similar principles in order to regulate vulnerability to chloride-assisted breakdown.

Acknowledgement

This manuscript was developed with primarily the support of the Office of Naval Research under MURI through Northwestern University #SP0028970-PROJ0007990-MURI ONR N00014-16-1-2280 (KLC). AYG and JRS were supported as part of the Center for Performance and Design of Nuclear Waste Forms and Containers, an Energy Frontier Research Center funded by the U.S. Department of Energy, Office of Science, Basic Energy Sciences under Award # DE-SC0016584 and all work on high entropy alloys derives from this support. Finally, CRD was supported by the Nuclear Energy University Program.

References

[1] J.R. Davis, ASM Specialty Handbook: Nickel, Cobalt, and Their Alloys, 2000. https://doi.org/10.1361/ncta2000p013.
[2] E. McCafferty, Introduction to Corrosion Science, Springer, 2010, https://doi.org/10.1007/978-1-4419-0455-3.
[3] K. Sugimoto, Y. Sawada, The role of molybdenum additions to austenitic stainless steels in the inhibition of pitting in acid chloride solutions, Corros. Sci. 17 (1977) 425–445, https://doi.org/10.1016/0010-938X(77)90032-4.
[4] M. Klimmeck, A study of the kinetics of passive layer formation on Cr-Mo alloys, Electrochim. Acta 25 (1980) 1375–1381.
[5] P.Y. Park, E. Akiyama, A. Kawashima, K. Asami, K. Hashimoto, The corrosion behavior of sputter-deposited Cr-Mo alloys in 12 M HCl solution, Corros. Sci. 37 (1995) 1843–1860, https://doi.org/10.1016/0010-938X(95)00090-7.
[6] J.B. Lumsden, Passivity of Metals: Proceedings of the Fourth International Symposium on Passivity, The Electrochemical Society, Princeton, NJ, 1978.
[7] R.B. Rebak, Corrosion and Environmental Degradiation, Weinheim, Germany, Germany, 2000.
[8] R.B. Rebak, Corrosion of non-ferrous alloys. I. Nickel-, Cobalt-, Copper-, Zirconium- and Titanium-based alloys, Mater. Sci. Technol. Wiley-VCH Verlag GmbH & Co. KGaA, Weinheim, Germany, 2013, pp. 71–111, , https://doi.org/10.1002/9783527603978.
[9] R.S. Lillard, M.P. Jurinski, J.R. Scully, Crevice corrosion of alloy-625 in chlorinated ASTM artificial ocean water, Corrosion 50 (1994) 251–265, https://doi.org/10.5006/1.3294331.
[10] R.M. Carranza, M.A. Rodríguez, Crevice corrosion of nickel-based alloys considered as engineering barriers of geological repositories, Npj Mater. Degrad. 1 (2017) 1–9, https://doi.org/10.1038/s41529-017-0010-5.
[11] A. Mishra, D. Shoesmith, P. Manning, Materials selection for use in concentrated hydrochloric acid, Corrosion 73 (2017) 68–76, https://doi.org/10.5006/2193.
[12] A.C. Lloyd, J.J. Noël, S. McIntyre, D.W. Shoesmith, Cr, Mo and W alloying additions in Ni and their effect on passivity, Electrochim. Acta 49 (2004) 3015–3027, https://doi.org/10.1016/j.electacta.2004.01.061.
[13] N. Ebrahimi, M.C. Biesinger, D.W. Shoesmith, J.J. Noël, The influence of chromium and molybdenum on the repassivation of nickel-chromium-molybdenum

alloys in saline solutions, Surf. Interface Anal. 49 (2017) 1359–1363, https://doi.org/10.1002/sia.6254.
[14] J.R. Scully, Future frontiers in corrosion science and engineering, Part II: Managing the many stages of corrosion, Corrosion 75 (2018) 123–125, https://doi.org/10.5006/3132.
[15] C.R. Clayton, Y.C. Lu, A bipolar model of the passivity of stainless steel: the role of Mo addition, J. Electrochem. Soc. 133 (1986) 2465–2473, https://doi.org/10.1149/1.2108451.
[16] P. Marcus, Corrosion Mechanisms in Theory and Practice, Third Edition - Google Books, third ed., CRC Press, 2012.
[17] A.C. Lloyd, J.J. Noël, N.S. McIntyre, D.W. Shoesmith, The open-circuit ennoblement of alloy C-22 and other Ni-Cr-Mo alloys, JOM 57 (2005) 31–35, https://doi.org/10.1007/s11837-005-0061-x.
[18] E.B. Haugan, M. Næss, C.T. Rodriguez, R. Johnsen, M. Iannuzzi, Effect of tungsten on the pitting and crevice corrosion resistance of Type 25Cr super duplex stainless steels, Corrosion 73 (2017) 53–67, https://doi.org/10.5006/2185.
[19] C.W. Kovach, J.D. Redmond, Correlation between the critical crevice temperature "Pre-Number", and long-term crevice corrosion data for stainless steels, NACE Annu. Conf. Corros. Show, National Association of Corrosion Engineers, New Orleans, 1993.
[20] B.a. Kehler, G.O. Ilevbare, J.R. Scully, Crevice corrosion stabilization and repassivation behavior of alloys 625 and 22, Corrosion 57 (2001) 1042–1065.
[21] G.S. Frankel, T. Li, J.R. Scully, Localized corrosion: passive film breakdown vs pit growth stability, J. Electrochem. Soc. 164 (2017) C180–C181, https://doi.org/10.1149/2.1381704jes.
[22] M.P.Q. Argañaraz, S.B. Ribotta, M.E. Folquer, L.M. Gassa, G. Benítez, M.E. Vela, R.C. Salvarezza, Ni-W coatings electrodeposited on carbon steel: chemical composition, mechanical properties and corrosion resistance, Electrochim. Acta 56 (2011) 5898–5903, https://doi.org/10.1016/j.electacta.2011.04.119.
[23] P. de Lima-Neto, A.N. Correia, R.A.C. Santana, R.P. Colares, E.B. Barros, P.N.S. Casciano, G.L. Vaz, Morphological, structural, microhardness and electrochemical characterisations of electrodeposited Cr and Ni-W coatings, Electrochim. Acta 55 (2010) 2078–2086, https://doi.org/10.1016/j.electacta.2009.11.037.
[24] E. McCafferty, Graph theory and the passivity of binary alloys, Corros. Sci. 42 (2000) 1993–2011, https://doi.org/10.1016/S0010-938X(00)00038-X.
[25] E. McCafferty, Oxide networks, graph theory, and the passivity of Ni-Cr-Mo ternary alloys, Corros. Sci. 50 (2008) 3622–3628, https://doi.org/10.1016/j.corsci.2008.09.006.
[26] H. Kaesche, Corrosion of Metals: Physiochemical Principles and Current Problems, first ed.,, Springer-Verlag, Berlin, 2003https://doi.org/10.1007/978-3-642-96038-3.
[27] L.F. Lin, C.Y. Chao, D.D. Macdonald, A point defect model for anodic passive films II. Chemical breakdown and pit initiation, J. Electrochem. Soc. 128 (1981) 1194–1198, https://doi.org/10.1149/1.2127592.
[28] D.D. Macdonald, Some personal adventures in passivity—a review of the point defect model for film growth, Russ. J. Electrochem. 48 (2012) 235–258, https://doi.org/10.1134/S1023193512030068.
[29] V. Maurice, H. Peng, L.H. Klein, A. Seyeux, S. Zanna, P. Marcus, Effects of molybdenum on the composition and nanoscale morphology of passivated austenitic stainless steel surfaces, Faraday Discuss. 180 (2015) 151–170, https://doi.org/10.1039/c4fd00231h.
[30] J.R. Scully, Corrosion chemistry closing comments: opportunities in corrosion science facilitated by operando experimental characterization combined with multi- scale computational modelling, Faraday Discuss. 180 (2015) 577–593, https://doi.org/10.1039/c5fd00075k.
[31] G. Frankel, G. Thornton, S. Street, T. Rayment, D. Williams, A. Cook, A. Davenport, S. Gibbon, D. Engelberg, C. Örnek, A. Mol, P. Marcus, D. Shoesmith, C. Wren, K. Yliniemi, G. Williams, S. Lyon, R. Lindsay, T. Hughes, J. Lützenkirchen, S.-T. Cheng, J. Scully, S.F. Lee, R. Newman, C. Taylor, R. Springell, J. Mauzeroll, S. Virtanen, S. Heurtault, J. Sullivan, Localised corrosion: general discussion, Faraday Discuss. 180 (2015) 381–414, https://doi.org/10.1039/C5FD90046H.
[32] M. Urquidi, D.D. Macdonald, Solute-vacancy interaction model and the effect of minor alloying elements on the initiation of pitting corrosion, J. Electrochem. Soc. 132 (1985) 555–558, https://doi.org/10.1149/1.2113886.
[33] X.X. Yu, A. Gulec, Q. Sherman, K. Lutton Cwalina, J.R. Scully, J.H. Perepezko, P.W. Voorhes, L.D. Marks, Nonequilibrium solute capture in passivating oxide films, Phys. Rev. Lett. 121 (2018) 145701.
[34] J.C. Baker, J.W. Cahn, Solute trapping by rapid solidification, Acta Metall. 17 (1969) 575–578, https://doi.org/10.1016/0001-6160(69)90116-3.
[35] M.J. Aziz, Model for solute redistribution during rapid solidification, J. Appl. Phys. 53 (1982) 1158–1168.
[36] P. Crook, Corrosion of Nickel and Nickel-Base Alloys, ASM Int. Mater. Park …. (n.d.).
[37] D.S. Dunn, Y.-M. Pan, L. Yang, G.A. Cragnolino, Localized corrosion susceptibility of alloy 22 in chloride solutions: Part 2—Effect of fabrication processes, Corrosion 62 (2006) 3–12, https://doi.org/10.5006/1.3278250.
[38] M. Raghavan, B.J. Berkowitz, J.C. Scanlon, Electron microscopic analysis of heterogeneous precipitates in hastelloy C-276, Metall. Trans. A 13 (1982) 979–984, https://doi.org/10.1007/BF02643394.
[39] D.S. Dunn, Y.-M. Pan, K.T. Chiang, L. Yang, G.A. Cragnolino, X. He, The localized corrosion resistance and mechanical properties of alloy 22 waste package outer containers, JOM 57 (2005) 49–55, https://doi.org/10.1007/s11837-005-0064-7.
[40] R.M. Carranza, M.A. Rodríguez, R.B. Rebak, Anodic And Cathodic Behavior Of Mill Annealed And Topologically Closed Packed Alloy 22 In Chloride Solutions, in: NACE International, New Orleans, 2008.
[41] A.K. Mishra, D.W. Shoesmith, Effect of alloying elements on crevice corrosion inhibition of nickel-chromium-molybdenum-tungsten alloys under aggressive conditions: an electrochemical study, Corrosion 70 (2014) 721–730, https://doi.org/10.5006/1170.
[42] A.K. Mishra, D.W. Shoesmith, The activation/depassivation of nickel-chromium-molybdenum alloys: An oxyanion or a pH effect – Part II, Electrochim. Acta 102 (2013) 328–335, https://doi.org/10.1016/j.electacta.2013.03.177.
[43] K.F. Quiambao, S.J. McDonnell, D.K. Schreiber, A.Y. Gerard, K.M. Freedy, P. Lu, J.E. Saal, G.S. Frankel, J.R. Scully, Passivation of a corrosion resistant high entropy alloy in non-oxidizing sulfate solutions, Acta Mater. 164 (2019) 362–376, https://doi.org/10.1016/J.ACTAMAT.2018.10.026.
[44] P. Lu, J.E. Saal, G.B. Olson, T. Li, O.J. Swanson, G.S. Frankel, A.Y. Gerard, K.F. Quiambao, J.R. Scully, Computational materials design of a corrosion resistant high entropy alloy for harsh environments, Scr. Mater. 153 (2018) 19–22, https://doi.org/10.1016/j.scriptamat.2018.04.040.
[45] S. Sosa, M.A. Rodriguez, R.M. Carranza, Determining the effect of the main alloying elements on localized corrosion in nickel alloys using artificial neural networks, Procedia Mater. Sci. 8 (2015) 21–28, https://doi.org/10.1016/j.mspro.2015.04.044.
[46] K. Gusieva, K.L. Cwalina, W.H. Blades, G. Ramalingam, J.H. Perepezko, P. Reinke, J.R. Scully, Repassivation behavior of individual grain facets on dilute Ni–Cr and Ni–Cr–Mo alloys in acidified chloride solution, J. Phys. Chem. C. 122 (2018) 19499–19513, https://doi.org/10.1021/acs.jpcc.8b04306.
[47] J.J. Gray, B.S. El Dasher, C.A. Orme, Competitive effects of metal dissolution and passivation modulated by surface structure: an AFM and EBSD study of the corrosion of alloy 22, Surf. Sci. 600 (2006) 2488–2494, https://doi.org/10.1016/j.susc.2006.04.002.
[48] D.J. Horton, A.W. Zhu, J.R. Scully, M. Neurock, Crystallographic controlled dissolution and surface faceting in disordered face-centered cubic FePd, MRS Commun. 4 (2014) 113–119, https://doi.org/10.1557/mrc.2014.23.
[49] E.C. Hornus, C.M. Giordano, M.a. Rodríguez, R.M. Carranza, R.B. Rebak, Effect of temperature on crevice corrosion susceptibility of nickel alloys for nuclear repositories, Corrosion 162 (2013) 1–13, https://doi.org/10.1149/2.0431503jes.
[50] R.B. Rebak, P. Crook, Influence of the environment on the general corrosion rate of alloy 22, Am. Soc. Mech. Eng. Press. Vessel. Pip. Devision Conf. 2004, pp. 1–8, , https://doi.org/10.1115/PVP2004-2793.
[51] J.R. Scully, K. Lutton, Polarization behavior of active passive metals and alloys, Encycl. Interfacial Chem. Surf. Sci Electrochem. (2018).
[52] I. Betova, M. Bojinov, P. Kinnunen, T. Laitinen, P. Pohjanne, T. Saario, Mechanism of transpassive dissolution of nickel-based alloys studied by impedance spectroscopy and rotating ring-disc voltammetry, Electrochim. Acta 47 (2002) 2093–2107, https://doi.org/10.1016/S0013-4686(02)00080-4.
[53] M. Bojinov, G. Fabricius, P. Kinnunen, T. Laitinen, K. Mäkelä, T. Saario, G. Sundholm, K. Yliniemi, Transpassive dissolution of Ni-Cr alloys in sulphate solutions – comparison between a model alloy and two industrial alloys, Electrochim. Acta 47 (2002) 1697–1712, https://doi.org/10.1016/S0013-4686(02)00018-X.
[54] M. Bojinov, G. Fabricius, P. Kinnunen, T. Laitinen, K. Mäkelä, T. Saario, G. Sundholm, Mechanism of transpassive dissolution of Ni-Cr alloys in sulphate solutions, Electrochim. Acta 45 (2000) 2791–2802, https://doi.org/10.1016/S0013-4686(00)00387-X.
[55] I. Betova, M. Bojinov, T. Tzvetkoff, Oxidative dissolution and anion-assisted solubilisation in the transpassive state of nickel-chromium alloys, Electrochim. Acta 49 (2004) 2295–2306, https://doi.org/10.1016/j.electacta.2004.01.010.
[56] M. Pourbaix, Atlas of electrochemical equilibria in aqueous solutions, Natl. Assoc. Corros. Eng. (1974).
[57] K. Lutton, J.R. Scully, Kinetics of oxide growth of passive films on transition metals, Encycl. Interfacial Chem. Surf. Sci. Electrochem. 6 (2018) 284–290.
[58] E.J. Verwey, Electrolytic conduction of a solid insulator at high fields: the formation of the anodic oxide film on aluminium, Physica 2 (1935) 1059–1063.
[59] N. Cabrera, N.F. Mott, Theory of the oxidation of metals, Rep. Prog. Phys. 12 (1949) 163–184, https://doi.org/10.1088/0034-4885/12/1/308.
[60] F.P. Fehlner, N.F. Mott, Low-temperature oxidation, Oxid. Met. 2 (1970) 59–99, https://doi.org/10.1007/BF00603582.
[61] C.Y. Chao, L.F. Lin, D.D. Macdonald, A point defect model for anodic passive films I. Film growth kinetics, J. Electrochem. Soc. 128 (1981) 1187–1194, https://doi.org/10.1149/1.2127591.
[62] M. Momeni, J.C. Wren, A mechanistic model for oxide growth and dissolution during corrosion of Cr-containing alloys, Faraday Discuss. 180 (2015) 1–23, https://doi.org/10.1039/C4FD00244J.
[63] K. Leistner, C. Toulemonde, B. Diawara, A. Seyeux, V. Maurice, P. Marcus, Oxide film growth kinetics on metals and alloys: II. Numerical simluation of transient behavior, J. Electrochem. Soc. 160 (2013) C197–C205, https://doi.org/10.1149/2.036306jes.
[64] B. Beverskog, M. Bojinov, A. Englund, P. Kinnunen, T. Laitinen, K. Mäkelä, T. Saario, P. Sirkiä, A mixed-conduction model for oxide films on Fe, Cr and Fe-Cr alloys in high-temperature aqueous electrolytes – I. Comparison of the electrochemical behaviour at room temperature and at 200 °C, Corros. Sci. 44 (2002) 1901–1921, https://doi.org/10.1016/S0010-938X(02)00008-2.
[65] B. Beverskog, M. Bojinov, P. Kinnunen, T. Laitinen, K. Mäkelä, T. Saario, A mixed-conduction model for oxide films on Fe, Cr and Fe-Cr alloys in high-temperature aqueous electrolytes – II. Adaptation and justification of the model, Corros. Sci. 44 (2002) 1923–1940, https://doi.org/10.1016/S0010-938X(02)00009-4.
[66] K. Lutton, K. Gusieva, N. Ott, N. Birbilis, J.R. Scully, Understanding multi-element alloy passivation in acidic solutions using operando methods, Electrochem. Commun. 80 (2017) 44–47, https://doi.org/10.1016/j.elecom.2017.05.015.

[67] A. Seyeux, V. Maurice, P. Marcus, Oxide film growth kinetics on metals and alloys: I. Physical model, J. Electrochem. Soc. 160 (2013) C189–C196, https://doi.org/10.1149/2.036306jes.

[68] M. Momeni, M. Behazin, J.C. Wren, Mass and Charge Balance (MCB) model simulations of current, oxide growth and dissolution during corrosion of Co-Cr alloy stellite-6, J. Electrochem. Soc. 163 (2016) C94–C105, https://doi.org/10.1149/2.0721603jes.

[69] T. Li, J.R. Scully, G.S. Frankel, Localized corrosion: passive film breakdown vs pit growth stability: Part II. A model for critical pitting temperature, J. Electrochem. Soc. 165 (2018) C484–C491, https://doi.org/10.1149/2.0591809jes.

[70] J. Srinivasan, C. Liu, R.G. Kelly, Geometric evolution of flux from a corroding one-dimensional pit and its implications on the evaluation of kinetic parameters for pit stability, J. Electrochem. Soc. 163 (2016) C694–C703, https://doi.org/10.1149/2.1221610jes.

[71] J. Srinivasan, R.G. Kelly, One-dimensional pit experiments and modeling to determine critical factors for pit stability and repassivation, J. Electrochem. Soc. 163 (2016) C759–C767, https://doi.org/10.1149/2.0651613jes.

[72] P. Jakupi, D. Zagidulin, J.J. Noël, D.W. Shoesmith, The impedance properties of the oxide film on the Ni-Cr-Mo Alloy-22 in neutral concentrated sodium chloride solution, Electrochim. Acta 56 (2011) 6251–6259, https://doi.org/10.1016/j.electacta.2010.07.064.

[73] D.A. Jones, Principles and Prevention of Corrosion, Prentice Hall, 1996.

[74] P. Marcus, V. Maurice, H.H. Strehblow, Localized corrosion (pitting): a model of passivity breakdown including the role of the oxide layer nanostructure, Corros. Sci. 50 (2008) 2698–2704, https://doi.org/10.1016/j.corsci.2008.06.047.

[75] F. Bocher, R. Huang, J.R. Scully, Prediction of critical crevice potentials for Ni-Cr-Mo alloys in simulated crevice solutions as a function of molybdenum content, Corrosion 66 (2010) 1–15, https://doi.org/10.5006/1.3430462.

[76] G.S. Frankel, L. Stockert, F. Hunkeler, H. Boehni, Metastable pitting of stainless steel, Corrosion 43 (1987) 429–436, https://doi.org/10.5006/1.3583880.

[77] W.J. Tobler, S. Virtanen, Effect of Mo species on metastable pitting of Fe18Cr alloys-a current transient analysis, Corros. Sci. 48 (2006) 1585–1607, https://doi.org/10.1016/j.corsci.2005.05.049.

[78] Y.F. Cheng, J.L. Luo, Comparison of the pitting susceptibility and semiconducting properties of the passive films on carbon steel in chromate and bicarbonate solutions, Appl. Surf. Sci. 167 (2000) 113–121, https://doi.org/10.1016/S0169-4332(00)00534-1.

[79] R.S. Lillard, Factors influencing the transition from metastable to stable pitting in single-crystal beryllium, J. Electrochem. Soc. 148 (2001) B1–B11, https://doi.org/10.1149/1.1344526.

[80] B. Ter-Ovanessian, N. Mary, B. Normand, Passivity breakdown of Ni-Cr alloys: from anions interactions to stable pits growth, J. Electrochem. Soc. 163 (2016) C410–C419, https://doi.org/10.1149/2.0381608jes.

[81] B.A. Kehler, J.R. Scully, Role of metastable pitting in crevices on crevice corrosion stabilization in Alloys 625 and 22, Corrosion 61 (2005) 665–684, https://doi.org/10.5006/1.3278202.

[82] J.R. Scully, Future frontiers in corrosion science and engineering, Part I, Corrosion 74 (2017) 3–4, https://doi.org/10.5006/2734.

[83] L.-F. Huang, M.J. Hutchison, R.J. Santucci, J.R. Scully, J.M. Rondinelli, Improved electrochemical phase diagrams from theory and experiment: the Ni-water system and its complex compounds, J. Phys. Chem. C. 121 (2017) 9782–9789, https://doi.org/10.1021/acs.jpcc.7b02771.

[84] J.G. Speight, N.A. Lange, Lange's Handbook of Chemistry, 17th ed., McGraw-Hill Education, New York, 2017.

[85] L.-F. Huang, J. Rondinelli, Electrochemical stabilities of Ni-based compounds from bulk to nanoscale dimensions, Bull. Am. Phys Soc. (2018).

[86] H. Mao, H.-L. Chen, Q. Chen, TCHEA1: A thermodynamic database not limited for "High Entropy" alloys, J. Phase Equilibria Diffus. (2017) 1–16, https://doi.org/10.1007/s11669-017-0570-7.

[87] C.D. Taylor, P. Lu, J. Saal, G.S. Frankel, J.R. Scully, Integrated computational materials engineering of corrosion resistant alloys, Npj Mater. Degrad. 2 (2018) 1–10, https://doi.org/10.1038/s41529-018-0027-4.

[88] M.A. Rodríguez, R.M. Carranza, R.B. Rebak, Passivation and depassivation of Alloy 22 in acidic chloride solutions, J. Electrochem. Soc. 157 (2010) C1–C8, https://doi.org/10.1149/1.3246790.

[89] R.B. Rebak, J.H. Payer, Passive corrosion behavior of alloy 22, 11th Int. High Lev. Radioact. Waste Manag. Conf. 2006, pp. 1–7.

[90] J.J. Gray, J.R. Hayes, G.E. Gdowski, B.E. Viani, C.A. Orme, Influence of solution pH, anion concentration, and temperature on the corrosion properties of Alloy 22, J. Electrochem. Soc. 153 (2006) B61–B67, https://doi.org/10.1149/1.2160433.

[91] P. Jakupi, J.J. Noël, D.W. Shoesmith, The evolution of crevice corrosion damage on the Ni-Cr-Mo-W alloy-22 determined by confocal laser scanning microscopy, Corros. Sci. 54 (2012) 260–269, https://doi.org/10.1016/j.corsci.2011.09.028.

[92] D. Zagidulin, X. Zhang, J. Zhou, J.J. Noël, D.W. Shoesmith, Characterization of surface composition on Alloy 22 in neutral chloride solutions, Surf. Interface Anal. 45 (2013) 1014–1019, https://doi.org/10.1002/sia.5204.

[93] A.C. Lloyd, D.W. Shoesmith, N.S. McIntyre, J.J. Noël, Effects of temperature and potential on the passive corrosion properties of alloys C22 and C276, J. Electrochem. Soc. 150 (2003) B120–B130, https://doi.org/10.1149/1.1554914.

[94] A.K. Mishra, S. Ramamurthy, M. Biesinger, D.W. Shoesmith, The activation/depassivation of nickel-chromium-molybdenum alloys in bicarbonate solution: Part I, Electrochim. Acta 100 (2013) 118–124, https://doi.org/10.1016/j.electacta.2013.03.161.

[95] E.-A. Cho, C.-K. Kim, J.-S. Kim, H.-S. Kwon, Quantitative analysis of repassivation kinetics of ferritic stainless steels based on the high field ion conduction model, Electrochim. Acta 45 (2000) 1933–1942, https://doi.org/10.1016/S0013-4686(99)00415-6.

[96] E. McCafferty, Relationship between graph theory and percolation approaches in the passivity of Fe–Cr binary alloys, J. Electrochem. Soc. 155 (2008) C501–C505, https://doi.org/10.1149/1.2958291.

[97] E. McCafferty, Oxide networks, graph theory, and the passivity of binary alloys, Corros. Sci. 44 (2002) 1393–1409, https://doi.org/10.1016/j.corsci.2008.09.006.

[98] K. Sieradzki, R.C. Newman, Percolation model for passivation in stainless steels, J. Electrochem. Soc. 133 (1986) 1979–1980, https://doi.org/10.1149/1.2109065.

[99] J.D. Henderson, X. Li, D.W. Shoesmith, J.J. Noël, K. Ogle, Molybdenum surface enrichment and release during transpassive dissolution of Ni-based alloys, Corros. Sci. 147 (2019) 32–40, https://doi.org/10.1016/j.corsci.2018.11.005.

[100] G. Ramalingam, P. Reinke, Growth of Ni and Ni-Cr alloy thin films on MgO(001): effect of alloy composition on surface morphology, J. Appl. Phys. 120 (2016), https://doi.org/10.1063/1.4971261.

[101] W.H. Blades, P. Reinke, From alloy to oxide: capturing the early stages of oxidation on Ni–Cr(100) alloys, ACS Appl. Mater. Interfaces 10 (2019) 43219–43229, https://doi.org/10.1021/acsami.8b15210.

[102] N. Ebrahimi, The Influence of Alloying Elements on The Crevice Corrosion Behaviour of Ni-Cr-Mo Alloys, The, University of Western, Ontario, 2015.

[103] P.I. Marshall, G.T. Burstein, Effects of alloyed molybdenum on the kinetics of repassivation on austenitic stainless steels, Corros. Sci. 24 (1984) 463–478, https://doi.org/10.1016/0010-938X(84)90071-4.

[104] S. Ogura, K. Sugimoto, Y. Sawada, Effects of Cu, Mo and C on the corrosion of deformed 18Cr-8Ni stainless steels in H_2SO_4/NaCl solutions, Corros. Sci. 16 (1976) 323–337, https://doi.org/10.1016/0010-938X(76)90118-9.

[105] J.R. Hayes, J.J. Gray, A.W. Szmodis, C.A. Orme, Influence of chromium and molybdenum on the corrosion of nickel-based alloys, Corrosion 62 (2006) 491–500, https://doi.org/10.5006/1.3279907.

[106] X. Zhang, D. Zagidulin, D.W. Shoesmith, Characterization of film properties on the NiCrMo Alloy C-2000, Electrochim. Acta 89 (2013) 814–822, https://doi.org/10.1016/j.electacta.2012.11.029.

[107] P. Marcus, On some fundamental factors in the effect of alloying elements on passivation of alloys, Corros. Sci. 36 (1994) 2155–2158, https://doi.org/10.1016/0010-938X(94)90013-2.

[108] X. Zhang, D.W. Shoesmith, Influence of temperature on passive film properties on Ni-Cr-Mo Alloy C-2000, Corros. Sci. 76 (2013) 424–431, https://doi.org/10.1016/j.corsci.2013.07.016.

[109] L. Luo, L. Zou, D.K. Schreiber, D.R. Baer, S.M. Bruemmer, G. Zhou, C.M. Wang, In-situ transmission electron microscopy study of surface oxidation for Ni-10Cr and Ni-20Cr alloys, Scr. Mater. 114 (2016) 129–132, https://doi.org/10.1016/j.scriptamat.2015.11.031.

[110] L. Luo, L. Zou, D.K. Schreiber, M.J. Olszta, D.R. Baer, S.M. Bruemmer, G. Zhou, C.-M. Wang, In situ atomic scale visualization of surface kinetics driven dynamics of oxide growth on a Ni–Cr surface, Chem. Commun. 52 (2016) 3300–3303, https://doi.org/10.1039/C5CC09165A.

[111] A. Takei, K. Nii, The growth process of oxide layers in the initial stage of oxidation of 80Ni-20Cr alloy, Trans. Japan Inst. Met. 17 (1976) 211–219.

[112] H. Luo, S. Gao, C. Dong, X. Li, Characterization of electrochemical and passive behaviour of Alloy 59 in acid solution, Electrochim. Acta 135 (2014) 412–419, https://doi.org/10.1016/j.electacta.2014.04.128.

[113] X. Yu, A. Gulec, C. Andolina, E. Zeitchick, K. Gusieva, J. Yang, J. Scully, J. Perepezko, L. Marks, P. Engineering, In-situ observations of early stage oxidation of Ni-Cr and Ni-Cr-Mo alloys, Corrosion 74 (2018) 939–946, https://doi.org/10.5006/2807.

[114] L. Luo, M. Su, P. Yan, L. Zou, D.K. Schreiber, D.R. Baer, Z. Zhu, G. Zhou, Y. Wang, S.M. Bruemmer, Z. Xu, C. Wang, Atomic origins of water-vapour-promoted alloy oxidation, Nat. Mater. 17 (2018) 514–518, https://doi.org/10.1038/s41563-018-0078-5.

[115] A.J. Davenport, B.K. Lee, Passive film growth kinetics for iron and stainless steel, Electrochem. Soc. Proc. 13 (2002) 187–197.

[116] A.J. Davenport, G.T. Burstein, Concerning the distribution of the overpotential during anodic oxide film growth, J. Electrochem. Soc. 137 (1990) 1496–1501.

[117] D.W. Yun, H.S. Seo, J.H. Jun, J.M. Lee, K.Y. Kim, Molybdenum effect on oxidation resistance and electric conduction of ferritic stainless steel for SOFC interconnect, Int. J. Hydrogen Energy 37 (2012) 10328–10336, https://doi.org/10.1016/j.ijhydene.2012.04.013.

[118] A.J. Samin, C.D. Taylor, First-principles investigation of surface properties and adsorption of oxygen on Ni-22Cr and the role of molybdenum, Corros. Sci. 134 (2018) 103–111, https://doi.org/10.1016/J.CORSCI.2018.02.017.

[119] K. Sugimoto, Y. Sawada, Role of alloyed molybdenum in austenitic stainless steels in the inhibition of pitting in neutral halide solutions, Corrosion 32 (1976) 347–352.

[120] M. Bojinov, G. Fabricius, T. Laitinen, K. Mäkelä, T. Saario, G. Sundholm, Influence of molybdenum on the conduction mechanism in passive films on iron-chromium alloys in sulphuric acid solution, Electrochim. Acta 46 (2001) 1339–1358, https://doi.org/10.1016/S0013-4686(00)00713-1.

[121] The Douglass, oxidation mechanism of dilute Ni-Cr alloys, Corros. Sci. 8 (1968) 665–678.

[122] D. Liang, W. Shao, G. Zangari, Selection of phase formation in electroplated Ag-Cu alloys, J. Electrochem. Soc. 163 (2016) 40–48, https://doi.org/10.1149/2.0651602jes.

[123] Y. Unutulmazsoy, R. Merkle, J. Mannhart, J. Maier, Chemical diffusion coefficient of Ni in undoped and Cr-doped NiO, Solid State Ionics 309 (2017) 110–117, https://doi.org/10.1016/j.ssi.2017.06.010.

[124] B.A. Kehler, G.O. Ilevbare, J.R. Scully, Comparison of the crevice corrosion resistance of alloys 625 and C22, Passiv. Localized Corros. Int. Symp. Honor Profr.

Norio Sato. 99 (1999) 644–654.
[125] R.W. Revie, H.H. Uhlig, Uhlig's Corrosion Handbook, third ed., WIley, 2011, https://doi.org/10.1002/9780470872864.ch49.
[126] C.F. Baes, R.E. Mesmer, The Hydrolysis of Cations, Wiley, New York, 1976.
[127] C.F. Baes, R.E. Mesmer, The thermodynamics of cation hydrolysis, Am. J. Sci. 281 (1981) 935–962, https://doi.org/10.2475/ajs.281.7.935.
[128] L. Marks, Competitive chloride chemisorption disrupts hydrogen bonding networks: DFT, Crystallogr. Thermodyn. Morphol. Conseq. Corros. 74 (2017) 295–311.
[129] B. MacDougall, Effect of chloride ion on the localized breakdown of nickel oxide films, J. Electrochem. Soc. 126 (1979) 919–925, https://doi.org/10.1149/1.2129194.
[130] P.M. Natishan, Perspectives on chloride interactions with passive oxides and oxide film breakdown, Corrosion (2017).
[131] J. Kunze, V. Maurice, L.H. Klein, H.H. Strehblow, P. Marcus, In situ STM study of the effect of chlorides on the initial stages of anodic oxidation of Cu(111) in alkaline solutions, Electrochim. Acta 48 (2003) 1157–1167, https://doi.org/10.1016/S0013-4686(02)00826-5.
[132] A. Bouzoubaa, B. Diawara, V. Maurice, C. Minot, P. Marcus, Ab initio modelling of localized corrosion: study of the role of surface steps in the interaction of chlorides with passivated nickel surfaces, Corros. Sci. 51 (2009) 2174–2182, https://doi.org/10.1016/j.corsci.2009.05.048.
[133] J.M. Kolotyrkin, Effects of anions on the dissolution kinetics of metals, J. Electrochem. Soc. 108 (1961) 209–216, https://doi.org/10.1149/1.2428048.
[134] A. Bouzoubaa, B. Diawara, V. Maurice, C. Minot, P. Marcus, Ab initio study of the interaction of chlorides with defect-free hydroxylated NiO surfaces, Corros. Sci. 51 (2009) 941–948, https://doi.org/10.1016/j.corsci.2009.01.028.
[135] A. Bouzoubaa, D. Costa, B. Diawara, N. Audiffren, P. Marcus, Insight of DFT and atomistic thermodynamics on the adsorption and insertion of halides onto the hydroxylated NiO(111) surface, Corros. Sci. 52 (2010) 2643–2652, https://doi.org/10.1016/j.corsci.2010.04.014.
[136] A. Seyeux, V. Maurice, L.H. Klein, P. Marcus, In situ STM study of the effect of chloride on passive film on nickel in alkaline solution, J. Electrochem. Soc. 153 (2006) B453–B463, https://doi.org/10.1149/1.2337768.
[137] D.D. Macdonald, The point defect model for the passive state, J. Electrochem. Soc. 139 (1992) 3434–3449, https://doi.org/10.1149/1.2069096.
[138] H.W. Pickering, Important early developments and current understanding of the IR mechanism of localized corrosion, J. Electrochem. Soc. 150 (2003) K1, https://doi.org/10.1149/1.1565142.
[139] B.A. Shaw, P.J. Moran, P.O. Gartland, The role of ohmic potential drop in the initiation of crevice corrosion on alloy 625 in seawater, Corros. Sci. 32 (1991) 707–719, https://doi.org/10.1016/0010-938X(91)90085-4.
[140] J.R. Galvele, Transport processes and the mechanism of pitting of metals, J. Electrochem. Soc. 123 (1976) 464, https://doi.org/10.1149/1.2132857.
[141] R.F. Steigerwald, A.P. Bond, H.J. Dundas, E.A. Lizlovs, The new Fe-Cr-Mo ferritic stainless steels, Corrosion 33 (1977) 279–295, https://doi.org/10.5006/0010-9312-33.8.279.
[142] R.C. Newman, The dissolution and passivation kinetics of stainless alloys containing molybdenum—II. Dissolution kinetics in artificial pits, Corros. Sci. 25 (1985) 341–350, https://doi.org/10.1016/0010-938X(85)90112-X.
[143] P. Jakupi, F. Wang, J.J. Noël, D.W. Shoesmith, Corrosion product analysis on crevice corroded Alloy-22 specimens, Corros. Sci. 53 (2011) 1670–1679, https://doi.org/10.1016/j.corsci.2011.01.028.
[144] A.K. Mishra, G.S. Frankel, Crevice corrosion repassivation of Alloy 22 in aggressive environments, Corrosion 64 (2008) 836–844, https://doi.org/10.5006/1.3279917.
[145] R.C. Newman, The dissolution and passivation kinetics of stainless alloys containing molybdenum—1. Coulometric studies of Fe-Cr and Fe-Cr-Mo alloys, Corros. Sci. 25 (1985) 331–339, https://doi.org/10.1016/0010-938X(85)90111-8.
[146] P. Wang, L.L. Wilson, D.J. Wesolowski, J. Rosenqvist, A. Anderko, Solution chemistry of Mo(III) and Mo(IV): thermodynamic foundation for modeling localized corrosion, Corros. Sci. 52 (2010) 1625–1634, https://doi.org/10.1016/J.CORSCI.2010.01.032.